The paradoxical lean phenotype of hypothyroid mice is marked by increased adaptive thermogenesis in the skeletal muscle

Rachel R. Kaspari[a], Andrea Reyna-Neyra[a], Lara Jung[a,1], Alejandra Paola Torres-Manzo[b], Sandro M. Hirabara[a,c,2], and Nancy Carrasco[a,b,3]

[a]Department of Cellular and Molecular Physiology, Yale School of Medicine, New Haven, CT 06510; [b]Department of Molecular Physiology and Biophysics, Vanderbilt University, Nashville, TN 37203; and [c]Department of Internal Medicine, Yale School of Medicine, New Haven, CT 06520

Contributed by Nancy Carrasco, July 22, 2020 (sent for review May 7, 2020; reviewed by Antonio C. Bianco and Gregory A. Brent)

Obesity is a major health problem worldwide, given its growing incidence and its association with a variety of comorbidities. Weight gain results from an increase in energy intake without a concomitant increase in energy expenditure. To combat the obesity epidemic, many studies have focused on the pathways underlying satiety and hunger signaling, while other studies have concentrated on the mechanisms involved in energy expenditure, most notably adaptive thermogenesis. Hypothyroidism in humans is typically associated with a decreased basal metabolic rate, lower energy expenditure, and weight gain. However, hypothyroid mouse models have been reported to have a leaner phenotype than euthyroid controls. To elucidate the mechanism underlying this phenomenon, we used a drug-free mouse model of hypothyroidism: mice lacking the sodium/iodide symporter (NIS), the plasma membrane protein that mediates active iodide uptake in the thyroid. In addition to being leaner than euthyroid mice, owing in part to reduced food intake, these hypothyroid mice show signs of compensatory up-regulation of the skeletal-muscle adaptive thermogenic marker sarcolipin, with an associated increase in fatty acid oxidation (FAO). Neither catecholamines nor thyroid-stimulating hormone (TSH) are responsible for sarcolipin expression or FAO stimulation; rather, thyroid hormones are likely to negatively regulate both processes in skeletal muscle. Our findings indicate that hypothyroidism in mice results in a variety of metabolic changes, which collectively lead to a leaner phenotype. A deeper understanding of these changes may make it possible to develop new strategies against obesity.

hypothyroidism | sodium/iodide symporter (NIS) | food intake | adaptive thermogenesis | sarcolipin

The thyroid hormones (THs; tri-iodothyronine [T_3] and thyroxine [T_4]) are crucial for the development of the central nervous system (CNS), lungs, and skeletal muscle. They also regulate basal metabolic rate (BMR) throughout life (1–4). TH biosynthesis relies on the active transport of iodide into the thyroid by the sodium/iodide symporter (NIS) (5), as iodine is an essential constituent of the THs. In a negative feedback loop, TH biosynthesis and release are promoted by thyroid-stimulating hormone (TSH), which is, in turn, negatively regulated by the THs (2–4). Once in the bloodstream, the THs reach virtually all tissues throughout the body, where the more biologically active form, T_3, predominantly interacts with nuclear TH receptors to both positively and negatively regulate gene transcription, which ultimately leads to the effects of these hormones (2). Sufficient consumption of iodide and adequate NIS function are required to maintain a euthyroid condition. Thus, patients with iodide-deficiency disorders or mutations in NIS that cause iodide transport defects, if untreated, develop hypothyroidism (a state defined by reduced levels of THs and increased levels of TSH in the serum) and even cognitive impairment (6–10).

Obesity, the result of an imbalance between energy input and energy expenditure (11, 12), is a serious health issue in the United States, as over 42% of US adults were considered obese in 2018, and this number is expected to continue to rise (13). Many studies have focused on trying to promote energy expenditure to combat obesity by stimulating adaptive thermogenesis (14–16). In humans, hypothyroidism is often associated with weight gain (17). In contrast, hypothyroid mice—whether their hypothyroidism is induced by drug treatment or genetically engineered—are consistently leaner than euthyroid mice (18–21). However, the mechanisms responsible for this lower body weight remain largely unexplored.

We have generated knockout (KO) mice for *Slc5a5*, the gene encoding NIS (22), a mouse model that makes it possible to study the metabolic effects of hypothyroidism without the potentially confounding effects of the drugs used to induce hypothyroidism in other models. Using *Slc5a5* KO mice, we have demonstrated that hypothyroid mice are leaner than controls, but the reason for their failure to gain weight remains unknown (20). As mentioned above, stimulation of adaptive thermogenesis has attracted a great deal of attention as a potential treatment for obesity. THs are generally thought to be pro-thermogenic

Significance

The rate of obesity is steadily increasing in the United States and around the world, which is a major health concern, as weight gain is strongly associated with many leading causes of death. Although recent findings have deepened our understanding of the mechanisms underlying obesity, there is still a lack of therapeutic targets for inducing weight loss. We have found that a drug-free mouse model of hypothyroidism is paradoxically leaner than euthyroid controls. Here, we show that hypothyroid mice consume less food and display strikingly higher levels of skeletal-muscle adaptive thermogenesis. Our findings yield insights into the physiological adaptations that occur in hypothyroidism and may eventually help bring to light new targets for promoting weight loss.

Author contributions: R.R.K. and N.C. designed research; R.R.K., A.R.-N., L.J., A.P.T.-M., and S.M.H. performed research; R.R.K., A.R.-N., L.J., A.P.T.-M., and N.C. analyzed data; and R.R.K. and N.C. wrote the paper.

Reviewers: A.C.B., University of Chicago; and G.A.B., David Geffen School of Medicine at the University of California Los Angeles.

The authors declare no competing interest.

[1]Present address: School of Medicine, Heidelberg University, Heidelberg 69120, Germany.

[2]Present address: Interdisciplinary Post-Graduate Program in Health Science, Cruzeiro do Sul University, Sao Paulo 08060-070, Brazil.

[3]To whom correspondence may be addressed. Email: nancy.carrasco@vanderbilt.edu.

This article contains supporting information online at https://www.pnas.org/lookup/suppl/doi:10.1073/pnas.2008919117/-/DCSupplemental.

First published August 21, 2020.

(23–27); as a result, much of the available information on the topic of thermogenesis regulation by the THs has been obtained from studies in which THs were administered to mice to generate peripheral or central hyperthyroidism (23–27). Here, in contrast, we have capitalized on our *Slc5a5* KO mice to determine the effects of low levels of THs on several metabolic parameters. These hypothyroid mice are leaner than euthyroid controls and exhibit reduced body weight, lean mass, and fat mass, owing in part to reduced caloric intake. Strikingly, our hypothyroid mice up-regulate skeletal-muscle adaptive thermogenesis—most likely as a compensatory mechanism—although they are still cold-intolerant. These results indicate that a series of physiological adaptations occur in hypothyroidism, which cumulatively lead to a leaner phenotype. Identifying these adaptations may enable us to develop novel strategies for combating obesity.

Results

The Low Caloric Intake of Hypothyroid Mice Contributes to Their Lean Phenotype. We investigated the metabolic alterations that occur in hypothyroidism, using our whole-body *Slc5a5* KO mouse model. These mice offer the key advantage that their hypothyroidism is not drug-induced. We have previously shown that when *Slc5a5* KO mice are fed a standard rodent-chow diet, which supplies 40 times the recommended daily amount of iodide for rodents (28), iodide is in such great excess that it enters the thyroid via routes other than NIS, which partially rescues TH biosynthesis (22). Therefore, all mice were kept on a chow diet (6 parts per million [ppm] iodide) for their first 8 wk of life to promote normal development. After 8 wk, *Slc5a5* KO mice were switched to an iodide-deficient diet (IDD; 0.02 ppm iodide), which renders such mice hypothyroid, and *Slc5a5* wild-type (WT) mice were switched to an iodide-sufficient diet (ISD; 6 ppm iodide) with the same nutrient composition as the IDD, such that these mice were used as euthyroid controls (*SI Appendix*, Fig. S1*A*). In agreement with our previous findings (20), *Slc5a5* KO mice on an IDD had lower serum levels of THs (T_3 [Fig. 1*A*] and T_4 [Fig. 1*B*]) and markedly higher serum TSH levels (Fig. 1*C*) than *Slc5a5* WT littermate controls fed an ISD.

Although our ISD and IDD are isocaloric, hypothyroid mice failed to gain body weight after being switched to an IDD (Fig. 1*D*). MRI showed that hypothyroid mice had less fat mass (Fig. 1*E*) and lean mass (Fig. 1*F*) than euthyroid controls and that most of the changes in the body weight of the hypothyroid mice were likely due to differences in lean mass (Fig. 1*G*). When fat and lean mass were normalized to body weight, fat mass was still reduced in hypothyroid mice, whereas the two groups had proportionally similar amounts of lean mass (*SI Appendix*, Fig. S1 *B* and *C*). Overall fat mass normalized to body weight increased in both groups over time, whereas lean mass decreased (*SI Appendix*, Fig. S1*D*). These results thus indicate that some component(s) of hypothyroid physiology promote a leaner phenotype.

Body weight is determined by the balance between nutrient intake and energy output. To determine what factor(s) might be contributing to the leaner phenotype of hypothyroid mice, we first investigated nutrient intake by monitoring the weekly food consumption of both groups of mice. One week after the switch to an IDD, hypothyroid mice consumed significantly less food than euthyroid mice at a level that remained stable, but lower, for the entire 2 mo of monitoring (Fig. 1*H*). Therefore, the hypothyroid state caused mice to eat less and, thus, be leaner than euthyroid mice.

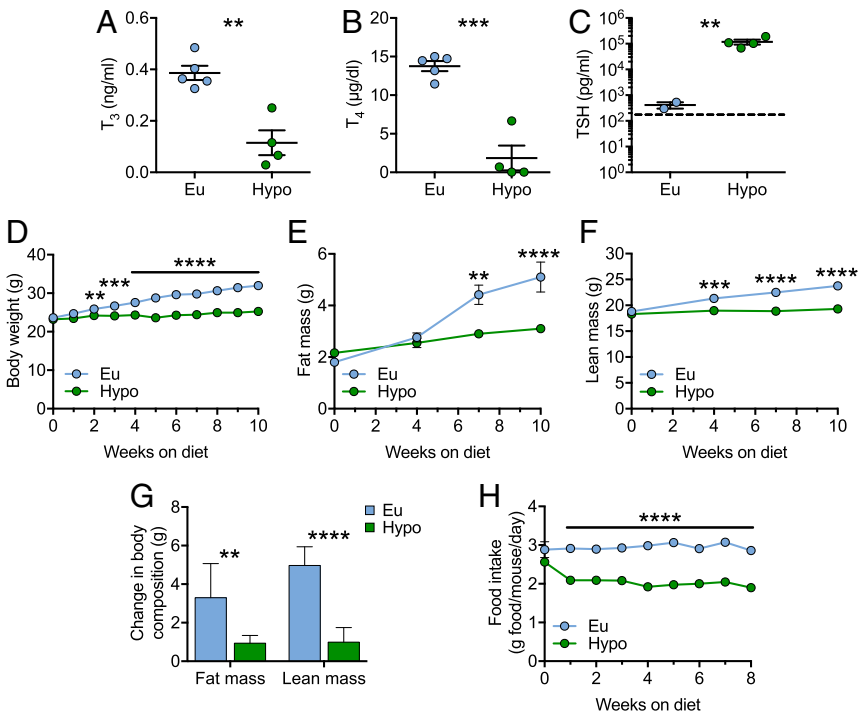

Fig. 1. Hypothyroid (Hypo) mice eat less and are leaner than euthyroid (Eu) controls. *Slc5a5* WT and KO mice were fed an ISD (6 ppm iodide) and IDD (0.02 ppm iodide), respectively, for 10 wk starting at 8 wk of age, rendering WT mice Eu and KO mice Hypo. (*A*–*C*) Serum T_3 (*A*), T_4 (*B*), and TSH (*C*) levels after 10 wk on special diet. For the TSH measurements, three Eu samples are below the detection limit of the assay, as depicted by the dotted line. Eu: $n = 5$; Hypo: $n = 4$. For *D*–*F* and *H*, week zero is a baseline measurement performed before the diet switch. (*D*) Weekly body weight of Hypo and Eu littermate controls. (*E* and *F*) MRI composition of fat mass (*E*) and lean mass (*F*). (*G*) Average fat mass and lean mass gained over 10 wk of special diet. (*H*) Weekly food intake of Hypo and Eu littermate controls. Eu: $n = 10$; Hypo: $n = 9$. Data are expressed as the mean ± SEM and were analyzed by an unpaired *t* test (*A*–*C* and *G*) or a two-way ANOVA followed by a Bonferroni correction (*D*–*F* and *H*). $^{**}P < 0.01$; $^{***}P < 0.001$; $^{****}P < 0.0001$.

Hypothyroidism Reduces Energy Expenditure and Activity. To quantitate energy expenditure, we performed a metabolic cage analysis on both groups of mice 10 wk after switching them to their respective diets. A striking pattern that emerged from the metabolic cage analysis is that energy expenditure by hypothyroid mice was shifted in time relative to that of euthyroid controls (Fig. 2*A*). These results suggest that the circadian rhythms of hypothyroid mice are altered. When we analyzed the energy-expenditure data using a nonlinear regression fit to a sine wave to quantitate rhythmicity, it emerged that euthyroid mice have a peak activity offset of approximately 2.3 h prior to the dark-cycle midpoint, whereas the circadian rhythms of hypothyroid mice were shifted by a remarkable 6.9 h. Such a large shift indicates that the active period is split evenly between the light and dark cycles in our hypothyroid mice. To better capture active and inactive periods in both groups of mice, we instead have analyzed the metabolic data synchronized with the active/inactive periodicity in each group. Overall, hypothyroid mice appear to expend less energy than euthyroid controls, with the most pronounced difference occurring during the active cycle (Fig. 2 *A* and *B*). Of note, the average resting energy expenditure, which is representative of BMR, was lower in hypothyroid mice during both the active and inactive cycles (*SI Appendix*, Fig. S2*A*). Consistent with a reduced energy expenditure, hypothyroid mice consumed less oxygen during both the active and inactive cycles (*SI Appendix*, Fig. S2*B*), but both groups had very similar respiratory quotients (*SI Appendix*, Fig. S2*C*).

We expect that the difference in body weight between the two groups (Fig. 1*D*) is a substantial contributor to the difference in energy expenditure between them (Fig. 2*A* and *B*). To quantitate energy expenditure and adjust for differences in body weight, we intended to perform an analysis of covariance (ANCOVA). However, our two experimental groups did not overlap in body weight, and the regression slopes were very different between groups (euthyroid: 0.0316; hypothyroid: −0.0389; *SI Appendix*, Fig. S2*D*), so an ANCOVA analysis could not be performed (29, 30). Thus, although some of the difference in energy expenditure between euthyroid and hypothyroid mice is probably related to body mass differences, we cannot quantitatively adjust for the body-mass variable. The regression analysis revealed that euthyroid mice exhibit an increase in energy expenditure at higher body weights—the expected phenotype—but, surprisingly, hypothyroid mice showed a decrease in energy expenditure with increased weight, which further supports the notion that there are fundamental differences in energy expenditure between hypothyroid mice and euthyroid controls.

To gain a better understanding of whether—and, if so, how—energy expenditure is altered in hypothyroid mice, we split it into its components: Total energy expenditure is the sum of the energy used for movement and the energy used to maintain core body temperature (i.e., used for thermogenesis). Total movement (Fig. 2 *C* and *D*) was drastically reduced in hypothyroid mice during the active cycle. In summary, our drug-free hypothyroid mice had a leaner phenotype than euthyroid mice, even though they exhibited classic signs of hypothyroidism, such as reduced energy expenditure and activity (2, 17, 21, 31).

Markers of Skeletal-Muscle Adaptive Thermogenesis Are Markedly Up-Regulated in Hypothyroid Mice. In addition to activity, we also investigated thermogenesis, the other main component of energy expenditure. The two groups of mice had very similar core body temperatures pre-diet—i.e., before the diet switch. However, after the *Slc5a5* KO mice were switched to an IDD to render them hypothyroid, their core body temperature decreased significantly, whereas that of the euthyroid controls did not (Fig. 3*A*). To differentiate more finely between the thermogenesis that occurs in euthyroid and hypothyroid mice, we investigated the main sites of adaptive thermogenesis: brown adipose tissue (BAT) and skeletal muscle. In BAT, the key mediator of adaptive thermogenesis is the inner mitochondrial membrane protein known as uncoupling protein 1 (UCP1) (32, 33). *Ucp1* messenger RNA (mRNA) levels were slightly higher in the BAT of hypothyroid than euthyroid mice (*SI Appendix*, Fig. S3*A*), and there was a trend toward higher UCP1 protein levels, but the difference was not statistically significant (*SI Appendix*, Fig. S3 *B* and *C*). Hematoxylin and eosin (H&E) staining of BAT from hypothyroid mice was more multilocular and showed fewer lipids than H&E staining of BAT from euthyroid mice, suggesting that there was moderate activation of thermogenesis in the BAT of hypothyroid mice (*SI Appendix*, Fig. S3*D*). In skeletal muscle, the small proteolipid sarcolipin, which uncouples calcium uptake into the sarcoplasmic reticulum from ATP hydrolysis by the sarco/endoplasmic reticulum calcium ATPase (SERCA), plays an important role in mediating adaptive thermogenesis (15, 34).

Both sarcolipin mRNA and protein levels were markedly higher in the soleus muscle of hypothyroid mice (Fig. 3 *B*–*D*). In agreement with previous results (35, 36), up-regulation of sarcolipin was limited to slow-twitch skeletal muscles: We detected increased expression in the diaphragms of hypothyroid mice (*SI Appendix*, Fig. S3 *E* and *F*), but no expression in either their gastrocnemius or their quadriceps (*SI Appendix*, Fig. S3 *G* and *H*).Using [^{14}C]-palmitate as a tracer, we found that the soleus muscles of hypothyroid mice produced more [^{14}C]-CO_2 (Fig. 3*E*) and [^{14}C]-acid-soluble metabolites (Fig. 3*F*), such as Krebs cycle intermediates that represent incomplete lipid oxidation, indicative of increased fatty acid oxidation (FAO). These results suggest that there is a pronounced stimulation of skeletal-muscle adaptive thermogenic mechanisms in hypothyroid mice, which may contribute to their leaner phenotype.

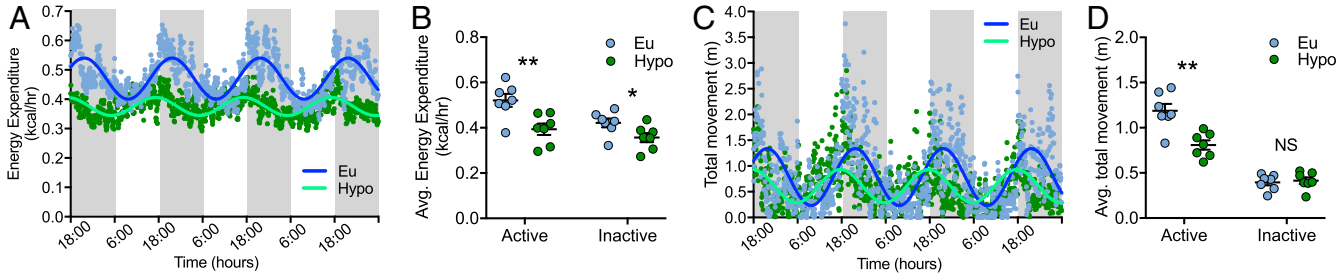

Fig. 2. Hypothyroid (Hypo) mice exhibit reduced energy expenditure and activity. Mice were fed their respective diets for 10 wk prior to a metabolic cage analysis. (*A* and *B*) Energy expenditure across the entire metabolic cage analysis (*A*) and averaged across the active/inactive cycles (*B*). (*C* and *D*) Total movement across the entire metabolic cage analysis (*C*) and averaged across the active/inactive cycles (*D*). $n = 7$ for both groups. Data in *A* and *C* represent the average across each group of metabolic readings collected at 5-min intervals that then underwent a nonlinear regression with a sine-function fit. Data in *B* and *D* represent the mean ± SEM and were analyzed by an unpaired *t* test. $^*P < 0.05$; $^{**}P < 0.01$. NS, not significant. Avg., average; Eu, euthyroid.

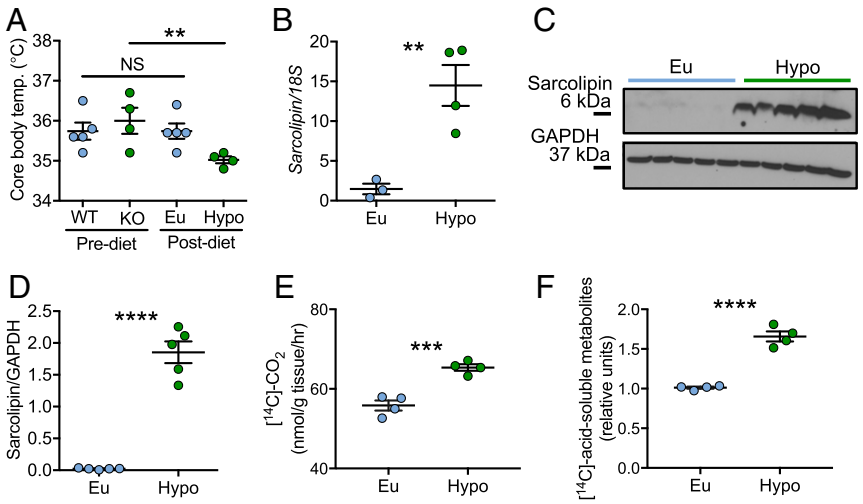

Fig. 3. Hypothyroid (Hypo) mice exhibit signs of stimulated skeletal-muscle adaptive thermogenesis. Mice were fed their respective diets for 10 wk. (*A*) Core body temperature (temp.) measured using a rectal probe before the diet switch (Pre-diet) and then after 10 wk on special diet (Post-diet). $n = 4$ for both groups. (*B* and *C*) Sarcolipin mRNA ($n = 3$ or 4) (*B*) and protein expression ($n = 5$) (*C*) in the soleus muscle. (*D*) Quantification of *C*. (*E* and *F*) Amount of [^{14}C]-CO_2 (*E*) and [^{14}C]-acid-soluble metabolites (*F*) produced by solei incubated in [^{14}C]-palmitate as a tracer. Data are expressed as the mean ± SEM and were analyzed by an unpaired *t* test. $^{**}P < 0.01$; $^{***}P < 0.001$; $^{****}P < 0.0001$. NS, not significant. Eu, euthyroid.

To investigate whether adaptive thermogenesis is stimulated in hypothyroid mice as a compensatory mechanism to help them maintain their core body temperature, we subjected the mice to a cold challenge. We placed euthyroid and hypothyroid mice at 4 °C and measured their core body temperature every 15 min. The core body temperature of the hypothyroid mice decreased dramatically as a result of the challenge, and they were therefore removed from the 4 °C environment after 135 min (Fig. 4*A*). Infrared imaging confirmed that, after 2 h at 4 °C, hypothyroid mice were clearly much colder than euthyroid controls (Fig. 4*B*). These results demonstrate that hypothyroid mice lack the metabolic mechanisms necessary to maintain their core body temperature in response to an extreme cold stress.

Interestingly, sarcolipin expression was still much higher in the soleus of hypothyroid than euthyroid mice after the cold challenge (Fig. 4 *C* and *D*), while UCP1 levels in the BAT of euthyroid and hypothyroid mice remained very similar (*SI Appendix*, Fig. S4 *A* and *B*). However, because the cold challenge lasted only a very short time (135 min), it is likely that these changes in protein expression occurred at room temperature, prior to the cold exposure. Consistent with this notion, sarcolipin expression levels in the soleus muscle (Fig. 4 *E* and *F*) and UCP1 levels in the BAT (*SI Appendix*, Fig. S4 *C* and *D*) were very similar in hypothyroid mice kept at room temperature and hypothyroid mice that underwent a cold challenge. These results show that hypothyroid mice were unable to maintain their core body temperature when placed at 4 °C, even though their UCP1 expression was similar to euthyroid controls and their skeletal muscle was "primed" for adaptive thermogenesis due to the increased sarcolipin expression, suggesting that other mechanisms, such as a reduced BMR, may be counteracting the increased adaptive thermogenesis. Furthermore, shivering is the first line of defense used to maintain core body temperature before adaptive thermogenic mechanisms are triggered (33). As our hypothyroid mice had to be removed from the cold challenge so quickly, their shivering may be impaired.

Neither TSH nor Catecholamine Signaling Play a Key Role in Hypothyroidism-Induced Sarcolipin Expression and Increased FAO. Very little is known concerning the regulation of sarcolipin expression. However, it is possible that the high levels of TSH in hypothyroid mice stimulate sarcolipin expression, as TSH has been implicated in BAT thermogenesis (specifically, restoring expression of the TSH receptor to the BAT of TSH receptor [*Tshr*] KO mice partially rescued thermogenesis; ref. 37). To ascertain whether or not elevated levels of TSH are directly responsible for increased sarcolipin expression, we used another mouse model of hypothyroidism: *Tshr* KO mice (38). As these mice lack the TSH receptor, they are unable to stimulate TH synthesis or release, making them markedly hypothyroid. *Tshr* WT control mice were kept on a chow diet (6 ppm iodide), whereas *Tshr* KO mice were kept on a 6 ppm iodide, TH-supplemented diet for the first 8 wk of life to promote normal development. After 8 wk, *Tshr* WT mice were placed on an ISD and were used as euthyroid controls, while *Tshr* KO mice were placed on an IDD and were used as a model of hypothyroidism (*SI Appendix*, Fig. S5*A*). As expected, *Tshr* KO mice had reduced serum levels of THs (T_3 [*SI Appendix*, Fig. S5*B*] and T_4 [*SI Appendix*, Fig. S5*C*]) and increased serum TSH levels (*SI Appendix*, Fig. S5*D*). Sarcolipin expression was higher in the solei of *Tshr* KO mice than *Tshr* WT mice (Fig. 5 *A* and *B*). Furthermore, sarcolipin up-regulation in hypothyroid mice correlated with higher levels of FAO in their soleus muscle (measured by using [^{14}C]-palmitate as a tracer). Solei from both hypothyroid mouse models (*Tshr* KO and *Slc5a5* KO) produced more [^{14}C]-CO_2 (Fig. 5*C*) and [^{14}C]-acid-soluble metabolites (Fig. 5*D*) than solei from euthyroid controls. These results show that signaling through the TSH receptor does not stimulate either sarcolipin expression or FAO.

It has been proposed that sympathetic nervous system (SNS) signaling may regulate skeletal-muscle adaptive thermogenesis and sarcolipin expression (39), owing to the role it plays in stimulating adipose-tissue adaptive thermogenesis (1, 16, 27, 33, 40, 41). In agreement with previous findings (42–44), catecholamine levels were higher in hypothyroid than in euthyroid mice after 10 wk on their respective diets (Fig. 6 *A* and *B*). To ascertain whether or not the elevated levels of catecholamines found in our hypothyroid mice were directly responsible for their increased sarcolipin expression, we quantitated the levels of plasma catecholamines in both groups at an earlier time point, with the rationale that SNS compensation may not yet have been triggered at that point. We have previously shown that *Slc5a5* KO

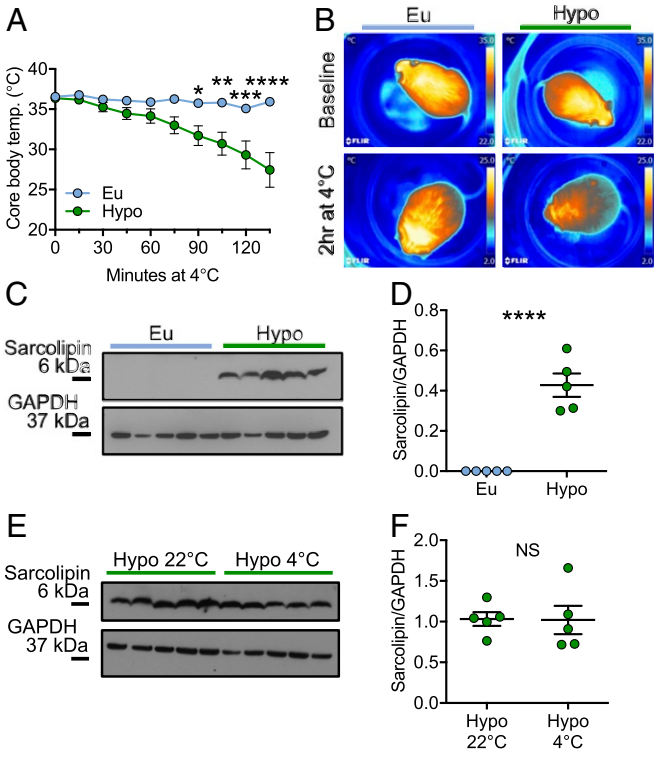

Fig. 4. Hypothyroid (Hypo) mice are severely cold-intolerant. Mice were housed at room temperature (22 °C) and fed their respective diets for 10 wk. They were then moved to 4 °C for a cold challenge. (*A*) Core body temperature (temp.) taken via temperature transponders. $n = 5$ for both groups. (*B*) Representative infrared images of a euthyroid (Eu) and a Hypo mouse before the cold challenge and after 2 h at 4 °C. (*C*) Sarcolipin protein expression in the soleus muscle of Eu and Hypo mice that underwent a cold challenge. (*D*) Quantification of *C*. (*E*) Sarcolipin protein expression in the soleus muscle of Hypo mice kept at room temperature (22 °C) or that underwent a cold challenge (4 °C). (*F*) Quantification of *E*. $n = 5$ for both groups. Data are expressed as the mean ± SEM. Data in *A* were analyzed by a two-way ANOVA followed by a Bonferroni correction. Data in *D* and *F* were analyzed by an unpaired *t* test. $^*P < 0.05$; $^{**}P < 0.01$; $^{***}P < 0.001$; $^{****}P < 0.0001$. NS, not significant.

mice are hypothyroid after only 3 wk on an IDD (20). As expected, after 4 wk on the IDD, *Slc5a5KO* mice were hypothyroid (*SI Appendix*, Fig. S5 *E–G*), but their plasma catecholamine levels (Fig. 6 *A* and *B*) were similar to those of the euthyroid controls, indicating that SNS compensation had not yet occurred. Sarcolipin expression, remarkably, was still up-regulated in the soleus muscle of hypothyroid mice under these conditions (Fig. 6 *C* and *D*). In addition, hypothyroid mice exhibited increased levels of [^{14}C]-CO_2 (Fig. 6*E*) and [^{14}C]-acid-soluble metabolites (Fig. 6*F*), strongly suggesting that hypothyroidism-induced sarcolipin expression and increased FAO do not depend on catecholamine signaling.

Discussion

Here, we show that hypothyroidism in mice triggers compensatory mechanisms that promote weight loss. We have reported that *Slc5a5* KO mice fed an IDD fail to gain body weight (20), a result that is in agreement with findings from drug-generated and genetically engineered mouse models of hypothyroidism (18, 19, 21). However, it is not well understood why they do not gain weight. Here, we have shown that hypothyroid mice are leaner than euthyroid controls, at least in part because they consume less food (Fig. 1*H*). In a centrally hyperthyroid rat model, activation of mammalian target of rapamycin (mTOR) signaling in the arcuate nucleus (ARC) of the hypothalamus was reported to increase feeding (45), and Coppola et al. (46) have shown that fasting stimulates local production of T_3 in the ARC to promote feeding through increased UCP2-mediated mitochondrial uncoupling. It can be inferred that the opposite occurs in hypothyroidism, as Coppola et al. (46) have reported decreased levels of hypothalamic *Ucp2* mRNA under hypothyroid conditions. Furthermore, increased SNS signaling has been associated with reduced food intake (47–49), suggesting that the elevated levels of catecholamines in our hypothyroid mice may also contribute to their decreased food consumption. Although the THs and SNS signal synergistically in other tissues (41), it has yet to be determined whether they signal together in the CNS to regulate food intake.

THs are key regulators of BMR throughout life (1–3), and hypothyroidism is often associated with a decreased BMR and lower energy expenditure. Our hypothyroid mice expend less energy and display less activity than euthyroid controls (Fig. 2 and *SI Appendix*, Fig. S2*A*)—typical manifestations of hypothyroidism. Our findings are consistent with results showing that hypothyroid mice and rats exhibit reduced running-wheel activity and energy expenditure (21, 31). These findings seem paradoxical, because they show that hypothyroid mice have a reduced body weight, despite phenotypic changes that conserve energy. However, our results differ from those authors' in that our hypothyroid mice, unlike theirs, displayed shifted circadian rhythms (Fig. 2 *A* and *C*). Cao et al. (50) showed that mTOR signals in the master circadian clock located in the suprachiasmatic nucleus (SCN) of the hypothalamus to regulate the expression of the clock proteins Period 1 and Period 2 to alter circadian rhythms. As mentioned above, THs regulate mTOR signaling in

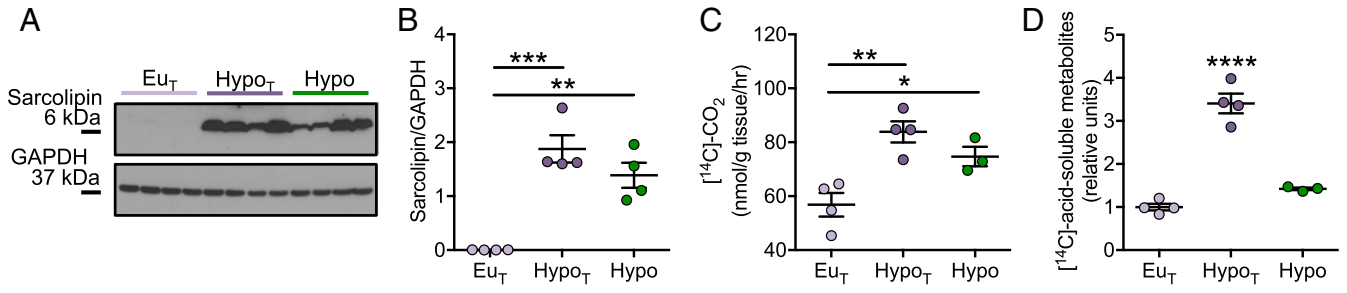

Fig. 5. TSH is not required for stimulation of sarcolipin expression and FAO. *Tshr* WT and KO mice were fed their respective diets for 4 wk, rendering WT mice euthyroid (Eu$_T$) and KO mice hypothyroid (Hypo$_T$). (*A*) Protein expression of sarcolipin in the soleus muscle. (*B*) Quantification of *A*. $n = 4$ for all groups. (*C* and *D*) Amount of [^{14}C]-CO_2 (*C*) and [^{14}C]-acid-soluble metabolites (*D*) produced by solei incubated in [^{14}C]-palmitate as a tracer. Eu$_T$: $n = 4$; Hypo$_T$: $n = 4$; Hypo: $n = 3$. Data are expressed as the mean ± SEM and were analyzed by a one-way ANOVA followed by a Tukey post hoc analysis. $^*P < 0.05$; $^{**}P < 0.01$; $^{***}P < 0.001$; $^{****}P < 0.0001$. Hypo, hypothyroid.

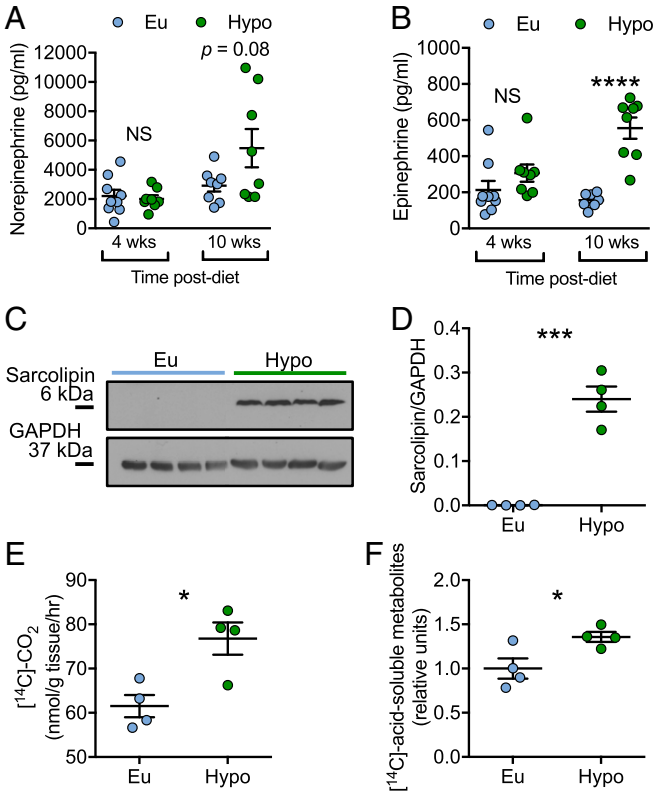

Fig. 6. Catecholamines are not required for stimulation of sarcolipin expression and FAO. (*A* and *B*) Plasma norepinephrine (*A*) and epinephrine (*B*) levels in euthyroid (Eu) and hypothyroid (Hypo) mice after 4 and 10 wk on either ISD or IDD, respectively. $n = 7$ to 9 for both groups. For *C–F*, mice were fed their respective diets for 4 wk. (*C*) Sarcolipin protein expression in the soleus muscle. (*D*) Quantification of *C*. $n = 4$ for both groups. (*E* and *F*) Amount of [^{14}C]-CO_2 (*E*) and [^{14}C]-acid-soluble metabolites (*F*) produced by solei incubated with [^{14}C]-palmitate as a tracer. $n = 4$ for both groups. Data are expressed as the mean ± SEM and were analyzed by an unpaired *t* test. $^*P < 0.05$; $^{***}P < 0.001$; $^{****}P < 0.0001$. NS, not significant.

the ARC to promote food intake (45); therefore, it seems plausible that hypothyroidism alters mTOR signaling in the SCN. However, it remains to be thoroughly investigated how TH disorders bring about metabolic and behavioral changes by altering circadian rhythms.

Stimulation of adaptive thermogenesis has recently emerged as a promising approach to promoting weight loss (14–16). THs are generally thought to be prothermogenic (1, 41, 51–53); as a consequence, most studies of THs have been carried out by using systemically (25–27) or centrally (23, 24) hyperthyroid animals. Here, in contrast, we studied hypothyroid mice, which displayed moderate activation of BAT thermogenesis (*SI Appendix*, Fig. S3 *A–D*) and pronounced stimulation of skeletal-muscle adaptive thermogenesis (Fig. 3 *B–F*), but were still severely cold-intolerant (Fig. 4 *A* and *B*). Our results indicate that some component of hypothyroidism, such as the reduction in BMR, interferes with the ability of these mice to maintain their core body temperature. Furthermore, our findings suggest that skeletal-muscle adaptive thermogenesis may play a more prominent role in TH-induced temperature alterations than does the adipose tissue. This is in agreement with recent results presented by Johann et al. (25) and Dittner et al. (26), who reported that hyperthyroidism triggers pyrexia without signaling through UCP1-dependent mechanisms.

Having found that neither TSH (Fig. 5) nor catecholamines (Fig. 6) are involved in sarcolipin regulation, we postulate that THs negatively regulate sarcolipin expression in skeletal muscle. Therefore, when TH levels are low, sarcolipin expression in the skeletal muscle increases. Consistent with this notion, Minamisawa et al. (54) proposed that THs accelerated sarcolipin mRNA degradation in the heart, and Johann et al. (25) recently reported that sarcolipin mRNA levels are lower in the soleus muscles of hyperthyroid than euthyroid mice. Finally, it has been known for decades that THs play an important role in calcium cycling in the skeletal muscle by stimulating expression of SERCA and the ryanodine receptor (Ryr) (1). Therefore, it seems highly plausible that the THs could also be involved in regulating sarcolipin expression and skeletal muscle metabolism.

Taken together, our findings suggest that the decreases in THs and BMR that occur in hypothyroid mice trigger compensatory mechanisms that, in turn, stimulate adaptive thermogenesis in an attempt to maintain core body temperature. These processes along with a reduced food intake ultimately result in a leaner phenotype. There is no question that the compensatory mechanisms triggered in hypothyroidism merit deep and sustained investigation, as they may eventually open up new avenues to combating obesity.

Materials and Methods

Animals. The Yale University Institutional Animal Care and Use Committee approved all mouse experiments. Mice were housed in a pathogen-free facility at Yale University on a 12-h light/dark cycle. All experiments were performed on male littermates housed at approximately 22 °C unless specified otherwise. Mice were fasted overnight prior to the FAO experiments and plasma collection for norepinephrine and epinephrine. The metabolic cage analysis was performed by Vanderbilt University's Mouse Metabolic Phenotyping Center (MMPC).

Slc5a5 KO mice on the C57BL/6J background were generated as described (22). We have shown that when *Slc5a5* KO mice are placed on a standard rodent-chow diet (ENVIGO catalog no. 2018S), which contains 40 times more iodide than the daily recommended amount for rodents (28), iodide is in such great excess that it enters the thyroid via nonspecific routes, which partially rescues TH biosynthesis (22). Therefore, *Slc5a5* KO mice develop normally and only become hypothyroid when placed on an IDD. To generate *Slc5a5* WT euthyroid and *Slc5a5* KO hypothyroid mice, all mice were given ad libitum access to a standard chow diet (6 ppm iodide; ENVIGO catalog no. 2018S) for the first 8 wk of life to promote normal development. After 8 wk, *Slc5a5* WT mice were switched to ad libitum access of an ISD (ENVIGO catalog no. TD.170762; 6 ppm iodide) to keep them euthyroid, whereas *Slc5a5* KO mice were switched to ad libitum access of an IDD (ENVIGO catalog no. TD.120723; 0.02 ppm iodide) to render them hypothyroid (*SI Appendix*, Fig. S1*A*). The ISD and IDD have the same nutrient composition and only differ in the amount of iodide supplied. Mice were fed their respective diets for either 4 or 10 wk, as specified in the text. *Slc5a5* euthyroid and hypothyroid mice are referred to as "Eu" and "Hypo," respectively, in the figures.

To generate *Tshr* euthyroid and hypothyroid mice, the following diet regimen was followed: *Tshr* WT mice were given ad libitum access to a standard rodent-chow diet (6 ppm iodide; ENVIGO catalog no. 2018S) for the first 8 wk of life before being switched to the ISD (ENVIGO catalog no. TD.170762; 6 ppm iodide) to keep them euthyroid. *Tshr* KO mice were given ad libitum access to a TH-supplemented diet (ENVIGO catalog no. TD.170763; 6 ppm iodide and 0.33 ppm levothyroxine) for the first 8 wk of life to keep them euthyroid throughout development. After 8 wk, *Tshr* KO mice were switched to ad libitum access of the IDD (ENVIGO catalog no. TD.120723; 0.02 ppm iodide) to render them hypothyroid (*SI Appendix*, Fig. S5*A*). Mice were fed their respective diets for 4 wk. *Tshr* euthyroid and hypothyroid mice are referred to as "Eu_T" and "$Hypo_T$," respectively in the figures.

Temperature Measurements. Rectal temperature measurements were performed by using a BIOSEB TK8851 rodent thermometer, while transponder measurements were performed by using programmable temperature transponders (IPTT-300; Bio Medic Data Systems). Transponders were injected at 6 wk of age into the subcutaneous region of the side body. Pre-diet measurements were conducted at 8 wk of age immediately prior to the switch to a special diet. Post-diet measurements were performed after 10 wk of special diet.

PHYSIOLOGY

Cold Challenge. Euthyroid and hypothyroid littermates were maintained at 22 °C for the first 18 wk of life. After 10 wk of either ISD or IDD, they were moved to 4 °C for a cold challenge. Core body-temperature measurements were made every 15 min by using programmable temperature transponders (IPTT-300; Bio Medic Data Systems), which were injected at 6 wk of age into the subcutaneous region of the side body. Mice were immediately removed from the cold challenge if their core body temperature fell below 30 °C. Infrared imaging was performed by using a FLIR T460 Thermal Imaging Camera with UltraMax Technology, and the FLIR Tools+ software was used for image analysis.

FAO. The soleus muscle was isolated from anesthetized mice and attached to a stainless-steel clip to keep the muscle under constant tension. Muscles were acclimated in an oxygenated Krebs–Ringer Bicarbonate Buffer (Sigma; catalog no. K4002) for 30 to 60 min in a shaking water bath at 35 °C. After acclimation, muscles were moved to a Krebs–Ringer Bicarbonate Buffer containing 0.1 mM total palmitate and 0.1 Ci/mL [1–^{14}C] palmitate for up to 6 h, followed by addition of HCl. NaOH at a concentration of 2 M was added into an isolated compartment in the incubation vial for $^{14}CO_2$ absorption. Finally, levels of [^{14}C]-CO_2 and [^{14}C]-acid soluble metabolites were determined by using a scintillation counter.

Hormone Measurements. The preservative ethylene glycol tetraacetic acid–glutathione was added to plasma for norepinephrine and epinephrine measurements immediately following collection. Samples were quickly spun down and stored at −80 °C until analysis. Norepinephrine and epinephrine levels were measured by high-performance liquid chromatography via electrochemical detection by the Vanderbilt University Medical Center (VUMC) Hormone Assay and Analytical Services Core. Similarly, T_3 was measured by using a radioimmunoassay by the VUMC Hormone Assay and Analytical Services Core. The Milliplex MAP Mouse Pituitary Magnetic Bead Panel was used to measure plasma T_4 (Millipore catalog no. RTHYMAG-30K) and TSH (Millipore catalog no. MPTMAG-49K). Both kits were used according to the manufacturer's instructions.

Real-Time PCR Analysis. Tissues for RNA extraction were immediately flash-frozen in liquid nitrogen upon dissection and stored at −80 °C until use. RNA was extracted by using TRIzol (Ambion catalog no. 15596018) and the RNeasy Mini Kit (Qiagen catalog no. 74104). Complementary DNA (cDNA) was synthesized by using the Quantabio qScript cDNA SuperMix kit (Quantabio catalog no. 95048) in accordance with the manufacturer's instructions. Amplification of cDNA was performed by using the Quantabio PerfeCTa SYBR Green FastMix (Quantabio catalog no. 95072) in accordance with the manufacturer's instructions and was performed on an Eco Real-Time PCR System (Illumina catalog no. 1010180). Gene expression was normalized to expression of the housekeeping gene *18S* run under the same conditions. Primer sequences were generated by using Primer-BLAST.

Western Blot Analysis. Tissues for Western blotting were immediately flash-frozen in liquid nitrogen upon dissection and stored at −80 °C until use. Both skeletal muscle and BAT tissue were homogenized in buffer containing 50 mM Tris·HCl (pH 7.5), 150 mM NaCl, 5 mM Na_3VO_4, 10 mM NaF, 2 mM protease inhibitor cocktail tablets cOmplete Mini, ethylenediaminetetraacetic acid-free (Roche catalog no. 11836170001), and 0.5% Nonidet P-40. Proteins were electrophoresed on an Invitrogen NuPAGE 4 to 12% Bis-Tris gel (Thermo Fisher Scientific) and transferred to a 0.2-μm nitrocellulose membrane (Bio-Rad catalog no. 1620112) using a Transblot SD semidry transfer cell (Bio-Rad catalog no. 221B). The membrane was probed with primary antibodies diluted 1:1,000 against sarcolipin (Millipore Sigma catalog no. ABT13) and 1:10,000 against UCP1 (Abcam catalog no. ab10983). Either a 1:10,000 dilution against GAPDH (Abcam catalog no. ab8245) or 1:1,000 dilution against cytochrome c oxidase subunit IV (COXIV). (Abcam catalog no. ab33985) was used as a loading control.

Statistical Analysis. Results were analyzed by using an unpaired *t* test, one-way ANOVA followed by a Tukey post hoc analysis, or a two-way ANOVA followed by a Bonferroni correction on GraphPad Prism 7 software. In Fig. 1*C* and *SI Appendix*, Fig. S5*G*, three and five of the TSH values for the euthyroid mice, respectively, were below the detection limit of the assay. For these analyses, the detection limit of the assay (180.74 pg/mL) was used as a substitute for the missing values. Data in all figures are expressed as means ± SEM. $*P < 0.05$; $**P < 0.01$; $***P < 0.001$; $****P < 0.0001$. NS indicates not significant.

To assess rhythmicity, we performed a nonlinear regression with a sine function fit using GraphPad Prism 7 software, obtaining 2.3- and 6.9-h phase shifts for euthyroid and hypothyroid mice, respectively. Active and inactive cycles were defined as 12-h periods accordingly phase-shifted from the dark/light cycle. The same active/inactive cycles were used for evaluation of all other metabolic parameters to permit comparison of parameters. (Independently determined phase shifts for the other parameters were very similar to those calculated for energy expenditure—total movement: 2.3 h for euthyroid and 6.3 h for hypothyroid; VO_2: 2.2 h for euthyroid and 6.8 h for hypothyroid; and respiratory quotient: 3.4 h for euthyroid and 7.9 h for hypothyroid).

Data Availability. All study data are included in the article and *SI Appendix*.

ACKNOWLEDGMENTS. We thank the members of the N.C. laboratory, Dr. Owen P. McGuinness, Dr. Biff Forbush, Dr. Louise Lantier, and Dr. Michael J. Caplan for their insightful comments and for helpful discussion. The *Tshr* KO mice were a generous gift from Dr. Terry Davies (Mount Sinai Medical Center, New York). This work was supported by NIH Grants DK041544 (to N.C.) and 1F31 DK118814-01A1 (to R.R.K.). The Vanderbilt MMPC performed the metabolic cage analysis. The MMPC is supported by NIH Grants DK059637 and 1S10RR028101-01. The VUMC Hormone Assay and Analytical Services Core is supported by NIH Grants DK059637 and DK020593.

1. J. E. Silva, Thermogenic mechanisms and their hormonal regulation. *Physiol. Rev.* **86**, 435–464 (2006).
2. R. Mullur, Y. Y. Liu, G. A. Brent, Thyroid hormone regulation of metabolism. *Physiol. Rev.* **94**, 355–382 (2014).
3. C. Portulano, M. Paroder-Belenitsky, N. Carrasco, The Na^+/I^- symporter (NIS): Mechanism and medical impact. *Endocr. Rev.* **35**, 106–149 (2014).
4. S. Ravera, A. Reyna-Neyra, G. Ferrandino, L. M. Amzel, N. Carrasco, The sodium/iodide symporter (NIS): Molecular physiology and preclinical and clinical applications. *Annu. Rev. Physiol.* **79**, 261–289 (2017).
5. G. Dai, O. Levy, N. Carrasco, Cloning and characterization of the thyroid iodide transporter. *Nature* **379**, 458–460 (1996).
6. O. Levy, C. Ginter, A. De La Vieja, D. Levy, N. Carrasco, Identification of a structural requirement for thyroid Na^+/I^- symporter (NIS) function from analysis of a mutation that causes human congenital hypothyroidism. *FEBS Lett.* **429**, 36–40 (1998).
7. J. Pohlenz, S. Refetoff, Mutations in the sodium/iodide symporter (NIS) gene as a cause for iodide transport defects and congenital hypothyroidism. *Biochimie* **81**, 469–476 (1999).
8. J. P. Nicola *et al.*, Iodide transport defect: Functional characterization of a novel mutation in the Na^+/I^- symporter 5′-untranslated region in a patient with congenital hypothyroidism. *J. Clin. Endocrinol. Metab.* **96**, E1100–E1107 (2011).
9. M. D. Reed-Tsur, A. De la Vieja, C. S. Ginter, N. Carrasco, Molecular characterization of V59E NIS, a Na^+/I^- symporter mutant that causes congenital I^- transport defect. *Endocrinology* **149**, 3077–3084 (2008).
10. Y. Watanabe, R. S. Ebrhim, M. A. Abdullah, R. E. Weiss, A novel missense mutation in the *SLC5A5* gene in a Sudanese family with congenital hypothyroidism. *Thyroid* **28**, 1068–1070 (2018).
11. B. M. Spiegelman, J. S. Flier, Obesity and the regulation of energy balance. *Cell* **104**, 531–543 (2001).
12. J. O. Hill, H. R. Wyatt, J. C. Peters, Energy balance and obesity. *Circulation* **126**, 126–132 (2012).
13. C. M. Hales, M. D. Carroll, C. D. Fryar, C. L. Ogden, Prevalence of obesity and severe obesity among adults: United States, 2017-2018 (NCHS Data Brief 360, National Center for Health Statistics, Hyattsville, MD, 2020).
14. H. M. Feldmann, V. Golozoubova, B. Cannon, J. Nedergaard, UCP1 ablation induces obesity and abolishes diet-induced thermogenesis in mice exempt from thermal stress by living at thermoneutrality. *Cell Metab.* **9**, 203–209 (2009).
15. N. C. Bal *et al.*, Sarcolipin is a newly identified regulator of muscle-based thermogenesis in mammals. *Nat. Med.* **18**, 1575–1579 (2012).
16. E. T. Chouchani, L. Kazak, B. M. Spiegelman, New advances in adaptive thermogenesis: UCP1 and beyond. *Cell Metab.* **29**, 27–37 (2019).
17. L. Chaker, A. C. Bianco, J. Jonklaas, R. P. Peeters, Hypothyroidism. *Lancet* **390**, 1550–1562 (2017).
18. C. B. Ueta, E. L. Olivares, A. C. Bianco, Responsiveness to thyroid hormone and to ambient temperature underlies differences between brown adipose tissue and skeletal muscle thermogenesis in a mouse model of diet-induced obesity. *Endocrinology* **152**, 3571–3581 (2011).
19. J. Weiner *et al.*, Thyroid hormone status defines brown adipose tissue activity and browning of white adipose tissues in mice. *Sci. Rep.* **6**, 38124 (2016).
20. G. Ferrandino *et al.*, Pathogenesis of hypothyroidism-induced NAFLD is driven by intra- and extrahepatic mechanisms. *Proc. Natl. Acad. Sci. U.S.A.* **114**, E9172–E9180 (2017).
21. K. Patyra *et al.*, Partial thyrocyte-specific $G\alpha_s$ deficiency leads to rapid-onset hypothyroidism, hyperplasia, and papillary thyroid carcinoma-like lesions in mice. *FASEB J.* **32**, 6239–6251 (2018).
22. G. Ferrandino *et al.*, An extremely high dietary iodide supply forestalls severe hypothyroidism in Na^+/I^- symporter (NIS) knockout mice. *Sci. Rep.* **7**, 5329 (2017).

23. M. Lopez *et al.*, Hypothalamic AMPK and fatty acid metabolism mediate thyroid regulation of energy balance. *Nat. Med.* **16**, 1001–1008 (2010).
24. N. Martinez-Sanchez *et al.*, Hypothalamic AMPK-ER stress-JNK1 axis mediates the central actions of thyroid hormones on energy balance. *Cell Metab.* **26**, 212–229.e12 (2017).
25. K. Johann *et al.*, Thyroid-hormone-induced browning of white adipose tissue does not contribute to thermogenesis and glucose consumption. *Cell Rep.* **27**, 3385–3400.e3 (2019).
26. C. Dittner, E. Lindsund, B. Cannon, J. Nedergaard, At thermoneutrality, acute thyroxine-induced thermogenesis and pyrexia are independent of UCP1. *Mol. Metab.* **25**, 20–34 (2019).
27. A. Guilherme *et al.*, Control of adipocyte thermogenesis and lipogenesis through β_3-adrenergic and thyroid hormone signal integration. *Cell Rep.* **31**, 107598 (2020).
28. National Research Council Subcommittee on Laboratory Animal Nutrition, *Nutrient Requirements of Laboratory Animals* (Nutrient Requirements of Domestic Animals, National Academy of Sciences, Washington, DC, ed. 4, 1995), pp. xii, 173.
29. A. I. Mina *et al.*, CalR: A web-based analysis tool for indirect calorimetry experiments. *Cell Metab.* **28**, 656–666.e1 (2018).
30. J. R. Speakman, Measuring energy metabolism in the mouse-theoretical, practical, and analytical considerations. *Front. Physiol.* **4**, 34 (2013).
31. L. P. Klieverik *et al.*, Thyroid hormone effects on whole-body energy homeostasis and tissue-specific fatty acid uptake in vivo. *Endocrinology* **150**, 5639–5648 (2009).
32. S. Enerback *et al.*, Mice lacking mitochondrial uncoupling protein are cold-sensitive but not obese. *Nature* **387**, 90–94 (1997).
33. B. Cannon, J. Nedergaard, Brown adipose tissue: Function and physiological significance. *Physiol. Rev.* **84**, 277–359 (2004).
34. N. C. Bal, S. K. Sahoo, S. K. Maurya, M. Periasamy, The role of sarcolipin in muscle non-shivering thermogenesis. *Front. Physiol.* **9**, 1217 (2018).
35. S. K. Maurya *et al.*, Sarcolipin signaling promotes mitochondrial biogenesis and oxidative metabolism in skeletal muscle. *Cell Rep.* **24**, 2919–2931 (2018).
36. G. J. Babu, P. Bhupathy, C. A. Carnes, G. E. Billman, M. Periasamy, Differential expression of sarcolipin protein during muscle development and cardiac pathophysiology. *J. Mol. Cell. Cardiol.* **43**, 215–222 (2007).
37. T. Endo, T. Kobayashi, Thyroid-stimulating hormone receptor in brown adipose tissue is involved in the regulation of thermogenesis. *Am. J. Physiol. Endocrinol. Metab.* **295**, E514–E518 (2008).
38. R. C. Marians *et al.*, Defining thyrotropin-dependent and -independent steps of thyroid hormone synthesis by using thyrotropin receptor-null mice. *Proc. Natl. Acad. Sci. U.S.A.* **99**, 15776–15781 (2002).
39. M. Pant, N. C. Bal, M. Periasamy, Sarcolipin: A key thermogenic and metabolic regulator in skeletal muscle. *Trends Endocrinol. Metab.* **27**, 881–892 (2016).
40. E. S. Bachman *et al.*, βAR signaling required for diet-induced thermogenesis and obesity resistance. *Science* **297**, 843–845 (2002).
41. J. E. Silva, S. D. Bianco, Thyroid-adrenergic interactions: Physiological and clinical implications. *Thyroid* **18**, 157–165 (2008).
42. L. Landsberg, J. Axelrod, Influence of pituitary, thyroid, and adrenal hormones on norepinephrine turnover and metabolism in the rat heart. *Circ. Res.* **22**, 559–571 (1968).
43. T. Tu, C. W. Nash, The influence of prolonged hyper- and hypothyroid states on the noradrenaline content of rat tissues and on the accumulation and efflux rates of tritiated noradrenaline. *Can. J. Physiol. Pharmacol.* **53**, 74–80 (1975).
44. P. Coulombe, J. H. Dussault, P. Walker, Plasma catecholamine concentrations in hyperthyroidism and hypothyroidism. *Metabolism* **25**, 973–979 (1976).
45. L. Varela *et al.*, Hypothalamic mTOR pathway mediates thyroid hormone-induced hyperphagia in hyperthyroidism. *J. Pathol.* **227**, 209–222 (2012).
46. A. Coppola *et al.*, A central thermogenic-like mechanism in feeding regulation: An interplay between arcuate nucleus T3 and UCP2. *Cell Metab.* **5**, 21–33 (2007).
47. G. A. Bray, Reciprocal relation of food intake and sympathetic activity: Experimental observations and clinical implications. *Int. J. Obes. Relat. Metab. Disord.* **24** (suppl. 2), S8–S17 (2000).
48. I. S. Racotta, M. Cabanac, L. Lafrance, Dissociation of anorectic and affective responses to epinephrine and glucose in rats. *Physiol. Behav.* **58**, 125–130 (1995).
49. C. S. Mantzoros *et al.*, Activation of β_3 adrenergic receptors suppresses leptin expression and mediates a leptin-independent inhibition of food intake in mice. *Diabetes* **45**, 909–914 (1996).
50. R. Cao, A. Li, H. Y. Cho, B. Lee, K. Obrietan, Mammalian target of rapamycin signaling modulates photic entrainment of the suprachiasmatic circadian clock. *J. Neurosci.* **30**, 6302–6314 (2010).
51. V. Golozoubova *et al.*, Depressed thermogenesis but competent brown adipose tissue recruitment in mice devoid of all hormone-binding thyroid hormone receptors. *Mol. Endocrinol.* **18**, 384–401 (2004).
52. M. Lopez, C. V. Alvarez, R. Nogueiras, C. Dieguez, Energy balance regulation by thyroid hormones at central level. *Trends Mol. Med.* **19**, 418–427 (2013).
53. J. Mittag, More than fever—novel concepts in the regulation of body temperature by thyroid hormones. *Exp. Clin. Endocrinol. Diabetes* **128**, 428–431 (2020).
54. S. Minamisawa *et al.*, Post-transcriptional downregulation of sarcolipin mRNA by triiodothyronine in the atrial myocardium. *FEBS Lett.* **580**, 2247–2252 (2006).